Expanded View Figures

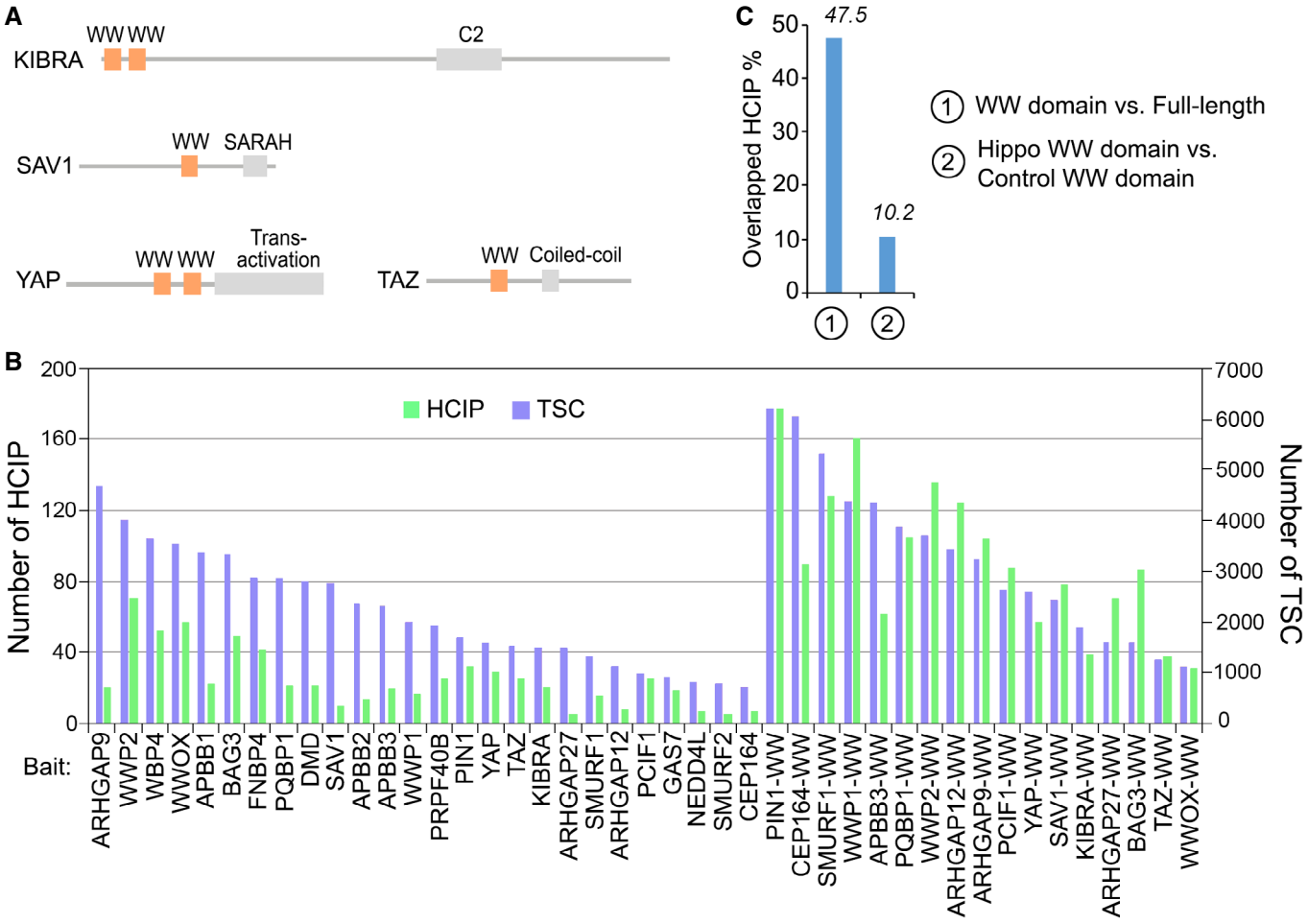

Figure EV1. Proteomic analysis of the WW-containing proteins. (This figure is related to Fig 1).

A Schematic illustration of the Hippo WW domain-containing components.

B The total spectral counts (TSCs) and corresponding numbers of HCIPs for the indicated proteomic experiments were listed.

C The overlapped HCIP rate was compared for the full-length protein vs. its WW domain, and Hippo WW domains vs. control WW domains, respectively.

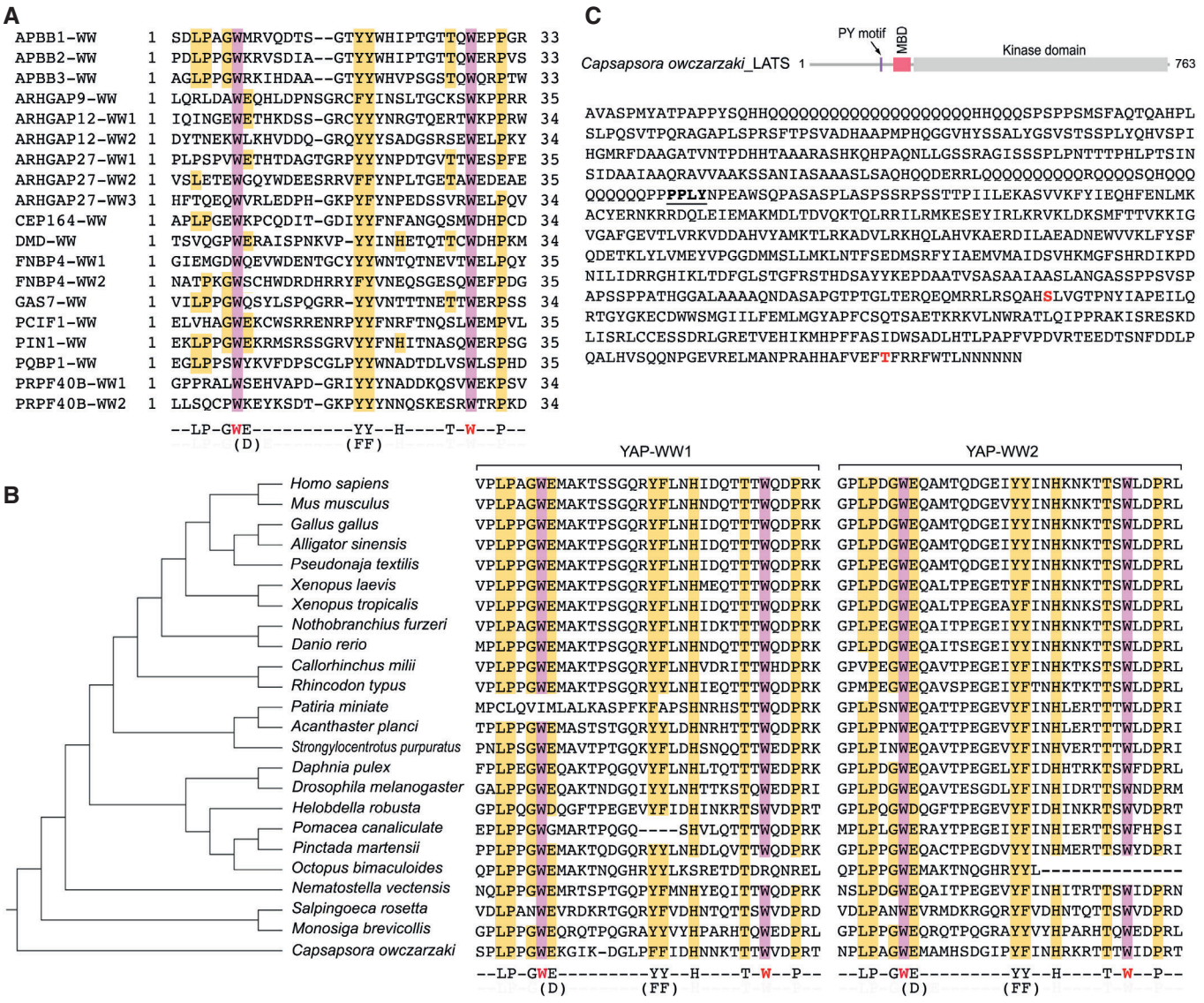

Figure EV2. Analyses of the identified 9-amino acid sequence in both control WW domains and evolution. (This figure is related to Fig 2; Appendix Figs S1 and S2; Table EV5).

A Sequence alignment of the WW domains derived from the control WW domain-containing proteins that cannot bind the Hippo PY motif-containing proteins. The two conserved tryptophan restudies were highlighted in purple, and the identified 9-amino acid residues were highlighted in yellow.

B Evolutionary analysis of the YAP-WW domains. The identified 9-amino acid sequence is highlighted in the two YAP-WW domains derived from the indicated species.

C A PY motif is identified in *Capsapsora owczarzaki* LATS. Schematic illustration of the *C. owczarzaki* LATS protein, where the PY motif is indicated. MBD, MOB1-binding domain. The PY motif is underlined in the *C. owczarzaki* LATS protein sequence, where the auto-phosphorylation site (S586) and the phosphorylation site (T750) in the hydrophobic motif were shown in red.

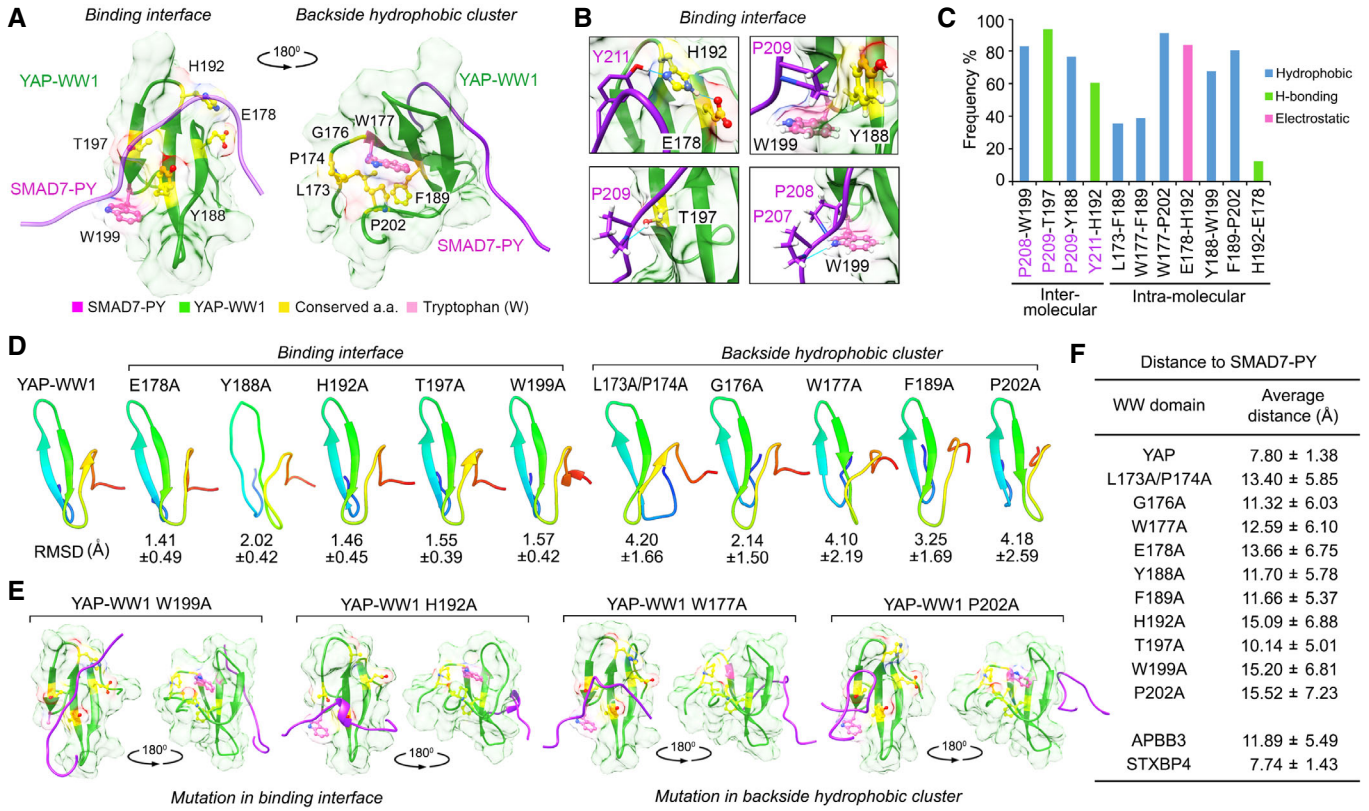

F

Distance to SMAD7-PY	
WW domain	Average distance (Å)
YAP	7.80 ± 1.38
L173A/P174A	13.40 ± 5.85
G176A	11.32 ± 6.03
W177A	12.59 ± 6.10
E178A	13.66 ± 6.75
Y188A	11.70 ± 5.78
F189A	11.66 ± 5.37
H192A	15.09 ± 6.88
T197A	10.14 ± 5.01
W199A	15.20 ± 6.81
P202A	15.52 ± 7.23
APBB3	11.89 ± 5.49
STXBP4	7.74 ± 1.43

Figure EV3. Structural analysis of the identified 9-amino acid sequence. (This figure is related to Fig 2 and Appendix Fig S3).

A Illustration of the identified 9-amino acid residues in the average YAP-WW1/SMAD7-PY structure. The initial structure was derived from NMR solution structure (2LTW). SMAD7-PY peptide was adjusted to 50% transparence to show the residue details on the binding interface.

B Four contact regions within the YAP-WW1/SMAD7-PY complex were shown in details from the representative top cluster structures. Residues from SMAD7-PY motif peptide were labeled in purple. Hydrogen bond is indicated in blue line.

C The binding type and the corresponding frequency rate were shown for the indicated inter- and intramolecular residue pairs.

D Simulation analysis of apo YAP-WW1 domain and its indicated mutants. RMSD value for each mutant simulation (referenced against the average apo YAP-WW1 domain) was shown.

E Average structures of the indicated YAP-WW1 mutant/SMAD7-PY complexes.

F The average distance between SMAD7-PY motif peptide and the indicated WW domains was summarized in a table.

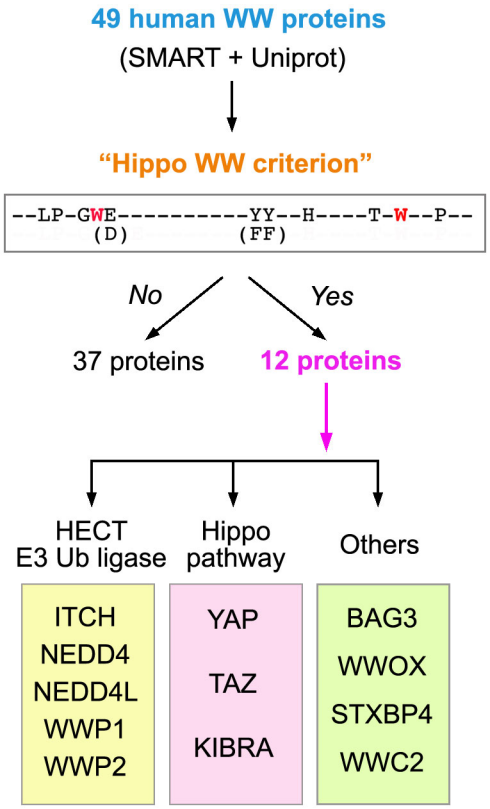

Figure EV4. Schematic illustration of the human proteome search for the WW domain-containing proteins that fit the Hippo WW domain 9-amino acid sequence criterion. (This figure is related to Fig 3; Table EV6).

The identified 9-amino acid sequence was subjected to the 49 WW domain-containing proteins in human proteome. Total 12 WW domain-containing proteins were found to contain the WW domains fitting the Hippo WW domain criterion.

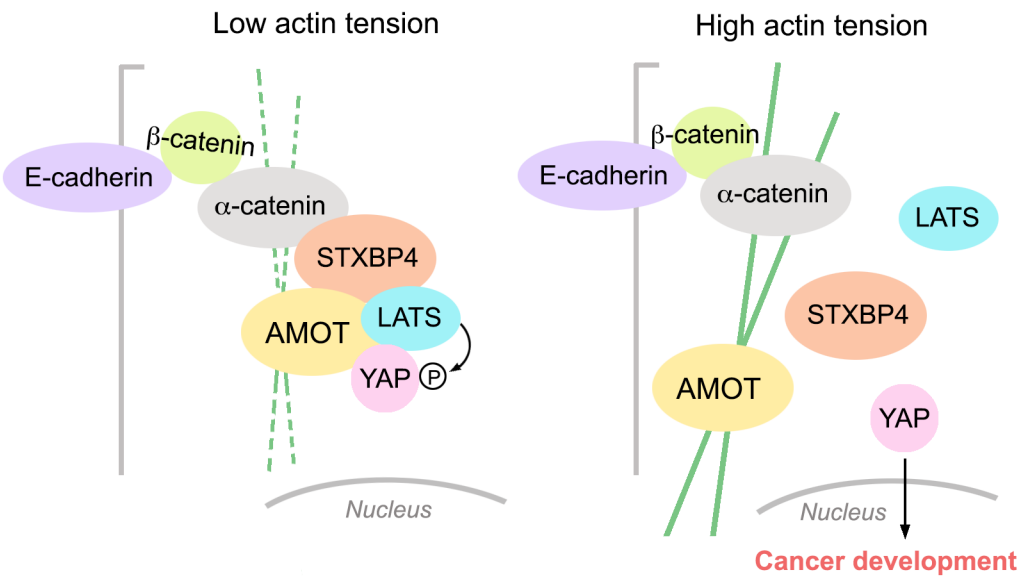

Figure EV5. A proposed model for the STXBP4-mediated Hippo pathway regulation in response to actin cytoskeleton tension change. (This figure is related to Figs 4 and 5).

Under low actin tension, STXBP4 assembles a protein complex comprising α-catenin, AMOT, LATS, and YAP to promote YAP phosphorylation and cytoplasmic retention. When actin cytoskeleton tension increases, the STXBP4-centered protein complex is dissembled, resulting in YAP's dephosphorylation and nuclear translocation as well as the subsequent cancer development.

© 2019 The Authors